Fiber coupling with adaptive optics for free-space optical communication

Thomas Weyrauch[a], Mikhail A. Vorontsov[a], John W. Gowens II[a], Thomas G. Bifano[b]
[a] U.S. Army Research Laboratory, Computational and Information Science Directorate,
2800 Powder Mill Road, Adelphi, MD 20783
[b] Boston University, Department of Manufacturing Engineering, Brookline, MA 02446

ABSTRACT

We describe an adaptive optical fiber coupling system for free-space optical communication comprising a micro-electromechanical deformable mirror and a VLSI gradient descent controller for model-free performance optimization. A comparison of Strehl ratio maximization with direct model-free coupling efficiency optimization revealed an advantage of the latter method.

Keywords: Laser communication, adaptive optics, model-free optimization

1. INTRODUCTION

Free-space laser communication (lasercom) systems are currently being considered for various applications, e. g. as an alternative for fiber optic links between buildings, reconfigurable and mobile communication links for military operations, or ground-satellite optical communication. Because of the high demands for the data transmission rates of communication systems, near future laser communication systems must work with wavelength division multiplexing (WDM). To keep the costs for free-space optical links between WDM fiber optical networks low, expensive multiplexing and demultiplexing systems at the transmitter and the receiver should be avoided. That means, a direct free-space optical connection from one fiber system to the other must be provided. A major problem for the use of lasercom systems, esp. for larger distances of several km, are the beam spreading and scintillations induced by the atmospheric turbulence, which cannot be compensated by increasing the optical power because of eye safety and power consumption limitations. A considerable improvement is expected using adaptive optics in the system that can correct (at least partially) the effects of turbulence[1].

Conventional adaptive optics systems are based on the wavefront conjugation principle. A schematic of an adaptive fiber-coupling receiver according to this approach is shown in Fig. 1. Phase conjugation is realized in an opto-electronic feedback-loop system comprising wavefront sensor and reconstructor, control system and deformable mirror. A basic problem of the phase conjugation principle for adaptive fiber coupling is that the real performance of the system, namely the optical power that is actually coupled into the fiber, is not used as a feedback signal. Several aspects of the coupling (to be discussed in Section 2), however, let expect that wavefront conjugation in general may not necessarily deliver the maximum coupling efficiency. This problem could be overcome using the model-free or blind optimization principle with the coupling efficiency (CE) as system performance metric. A schematic of a receiver system based on this principle using CE as single, scalar feedback parameter is shown in Fig. 2.

The difficulty to control a deformable mirror with a number of controllable elements up to the order of magnitude of hundreds with a single scalar feedback signal was a serious obstacle for the use of model-free optimization in real-time adaptive optics systems.[2] The information necessary to control individual mirror elements has to be acquired in time or frequency domain from a single sensor rather than from parallel signals of spatially distributed sensor arrays. Thus, the bandwidth of deformable mirror and controller required for real-time correction of atmospheric wave-front distortion was beyond the limitation of available hardware. Recent scientific and engineering progress changed the situation: Micro-machined deformable mirrors (μDMs) with high bandwidth, the development of the fast converging stochastic parallel gradient descent (SPGD) algorithm[3], its application for adaptive optics[4] and implementation in a VLSI controller (*AdOpt* system)[5,6] have given model-free adaptive optics a new perspective. For the *AdOpt* VLSI system iteration rates of up to 7000/sec were reported in previous papers[7,8]. A recent improvement of the system made iteration rates of 10 kHz and more possible (limited by the bandwidth of current μDMs) and allows for reasonable closed-loop bandwidths.

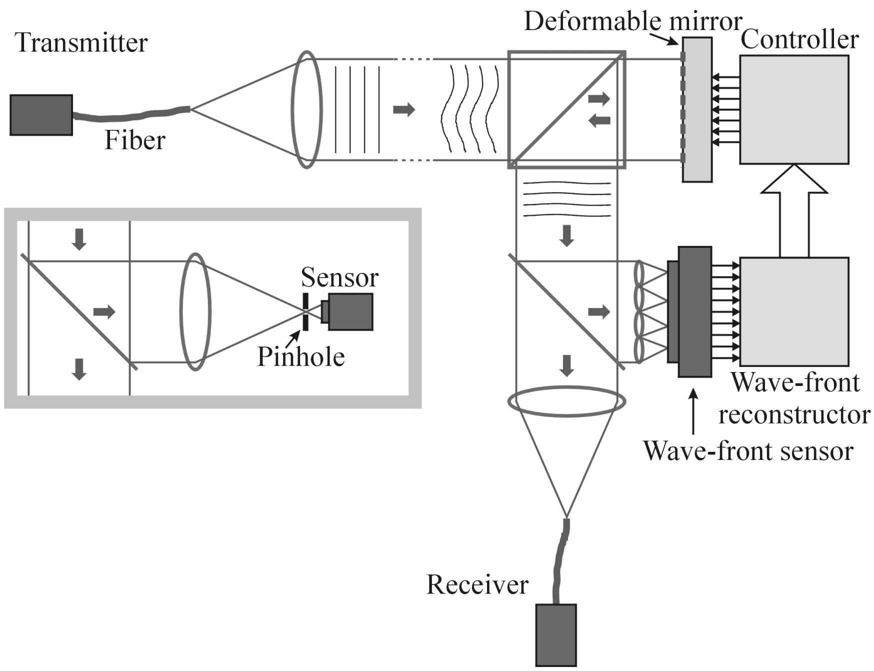

Figure 1: Free-space optical communication link with fiber coupling receiver based on conventional adaptive optics using wave-front sensor and reconstructor.

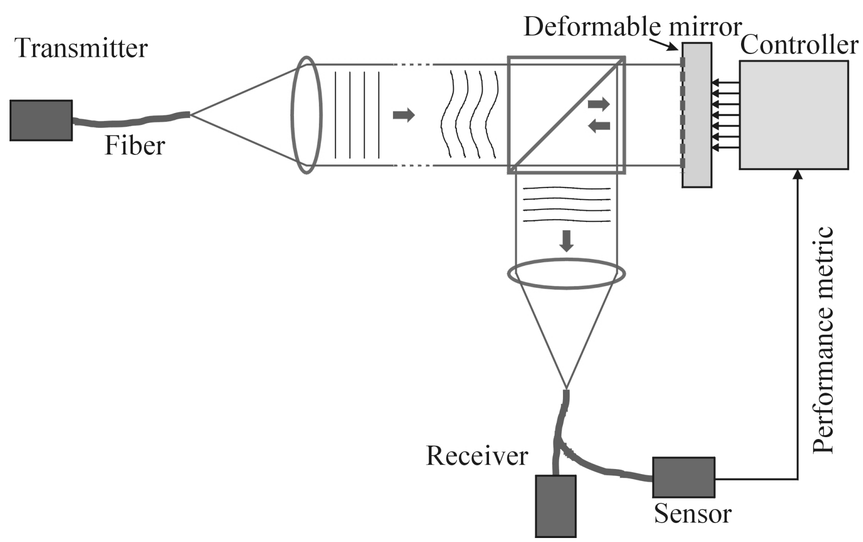

Figure 2: Free-space optical communication link with adaptive fiber coupling receiver based on model-free optimization.

Plett *et al.* reported recently fiber-coupling optimization by means of the SPGD algorithm using a comparable slow system with a personal computer as controller and a 37-control-channels membrane mirror.[9] No comparison of the direct optimization of the coupling efficiency with conventional adaptive optics was performed. Since model-free optimization allows for direct CE maximization as well as modeling of phase conjugation, we are able to perform a comparison of both approaches with one system. First results are presented in this paper.

2. PERFORMANCE METRICS FOR STREHL RATIO MAXIMIZATION AND DIRECT COUPLING EFFICIENCY OPTIMIZATION

The goal of a conventional adaptive optics system is to minimize the residual phase aberrations after the incoming wave passed the deformable mirror. This corresponds to a maximization of the Strehl ratio *St*, i.e. the ratio of the actual maximum intensity of the zero order diffraction spot and its theoretical upper limit for an undistorted wave. This is similar to model-free optimization, if the Strehl ratio is chosen as the system performance metric J_{St}.

$$J_{St} \equiv St \propto \left|A(\boldsymbol{r}_0)\right|^2 \ , \tag{1}$$

where $A(\boldsymbol{r})$ is the (complex) optical field in the focal plane and $\boldsymbol{r}_0$ is the desired on-axis location of the center of the fiber end within this plane. For model-free optimization it would be sufficient to measure a quantity that is (at least approximately) proportional to *St*, e.g. by replacing the wavefront sensor in Fig. 1 by a focusing lens, a pinhole, and a photodetector to measure the optical power emerging from the pinhole (cf. inset of Fig. 1). The measured quantity is thus proportional to the integral of the intensity within the pinhole with radius *a*, and we have an experimental performance metric

$$J_{St}^{exp} \propto \iint\limits_{|\boldsymbol{r}-\boldsymbol{r}_0|<a} \left|A(\boldsymbol{r})\right|^2 \, \mathrm{d}^2\boldsymbol{r} \ , \tag{2}$$

which is an acceptable approximation if *a* is not larger than the radius of the diffraction limited Airy disk.

For direct optimization of the power coupled into a fiber, the system performance metric J_{CE} is proportional to the absolute coupling efficiency. In case of a single-mode, the theoretical value is proportional to the overlap integral of the optical field $A(\boldsymbol{r})$ and the mode profile $M_0(\boldsymbol{r})$ in the focal plane,[10] thus the performance metric J_{CE} is given by

$$J_{CE}^{SM} \propto \frac{\left|\iint A(\boldsymbol{r}) M_0^*(\boldsymbol{r})\,\mathrm{d}^2\boldsymbol{r}\right|^2}{\iint A(\boldsymbol{r}) A^*(\boldsymbol{r})\,\mathrm{d}^2\boldsymbol{r} \times \iint M_0(\boldsymbol{r}) M_0^*(\boldsymbol{r})\,\mathrm{d}^2\boldsymbol{r}} \tag{3}$$

Both, $A(\boldsymbol{r})$ and $M_0(\boldsymbol{r})$ are complex quantities; therefore the intensity distribution as well as the phase of the optical field have to be considered for the maximization of the fiber coupling efficiency. Additional phase aberrations induced in the focal plane, e.g. due to a non-ideal shaped fiber end or due to imperfect polishing, may modify the optical field in the focal plane and thus impact the fiber coupling. In the case of coupling into multi-mode fibers the overlap integrals of the optical field with all N_M guided modes contribute to the overall coupling efficiency:

$$J_{CE}^{MM} \propto \frac{\sum_{i=0}^{N_M} \left|\iint A(\boldsymbol{r}) M_i^*(\boldsymbol{r})\,\mathrm{d}^2\boldsymbol{r}\right|^2}{\iint A(\boldsymbol{r}) A^*(\boldsymbol{r})\,\mathrm{d}^2\boldsymbol{r} \times \sum_{i=0}^{N_M} \iint M_i(\boldsymbol{r}) M_i^*(\boldsymbol{r})\,\mathrm{d}^2\boldsymbol{r}} \tag{4}$$

Moreover, the measured coupling efficiency may also not only depend on the situation on the fiber end but also on the propagation within the fiber, e.g. because of mode coupling.

The differences in the performance metrics for *St* maximization and CE optimization are illustrated in Fig. 3. The Strehl ratio metric J_{St} (Eq. 1) considers only the absolute value of the on-axis optical field, thus only the intensity at the location $\boldsymbol{r}_0$ in the focal plane but not the phase is relevant. In contrast, the performance metrics for CE optimization depend on both, intensity and phase distribution in the focal plane. An additional problem with conventional adaptive optics is, that one can't measure the Strehl ratio at the location of the fiber end but in a conjugate plane in another partial beam. Due to misalignment of the two subsystems (focusing onto the fiber end, Strehl ratio maximization) a pointing error may exist, that can severely degrade the system performance if the optical power coupled to the fiber is not used as a feedback signal.

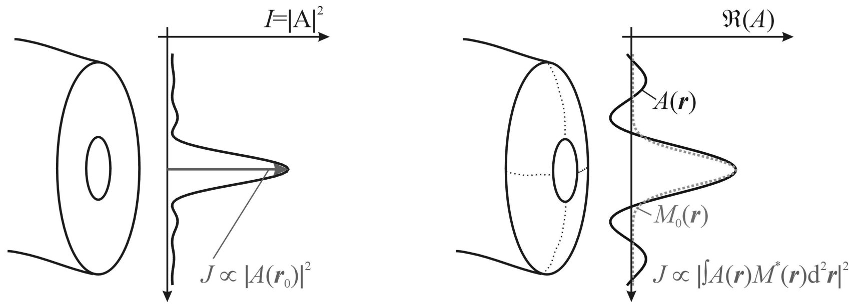

Figure 3: System performance criteria for Strehl ratio maximization (left) and power coupling efficiency optimization (right).

3. EXPERIMENTAL SET-UP

A schematic of the set-up used in the experiments is shown in Fig. 4. The collimated beam of a laser diode (λ = 690nm) was reflected from the µDM and redirected by the beam splitter BS1. After splitting the beam by BS2 one partial beam was focused onto a fiber end by lens L1, the other onto a pinhole by lens L2. The optical power in the pinhole as well as the power coupled into the fiber was measured by a photomultiplier module with integrated amplifier (PM1 and PM2, respectively). Both signals were acquired simultaneously by a personal computer and either one of them used as performance metric for the *AdOpt* VLSI controller. The *AdOpt* system implements a stochastic parallel gradient descent algorithm and has been described in detail in references 5, 6, and 8. The control voltage output channels are connected to a set of high voltage amplifiers in order to provide the 0 – 200 V input voltage range of the µDM.

The µDM (cf. Fig. 5a) from Boston University / Boston Micromachines Corporation has 140 actuators on a 12×12 grid (without the corner elements). The pitch is 300 µm; thus the whole mirror area of 11×11 segments is 3.3×3.3 mm^2. Four elements of the segmented membrane are connected to one actuator via a post allowing for tip-tilt control of the segments (cf. Fig. 5b). The *AdOpt* controller board in its current form uses seven chips with 19 control channels each, i.e. it provides a maximum of 133 channels. Thus, not all of the 140 actuators of the µDM could be controlled and 2 additional actuators in each corner were not used. This reduction of the number of controllable channels to 132 is insignificant considering a circular beam shape, as shown in the schematic in Fig. 5c, where the active actuators are depicted as black filled circles and the fully controlled part of the mirror membrane is shown as shaded area.

For a proper mutual alignment of the two subsystems (fiber coupler and pinhole) the *AdOpt* controller was used to optimize the power in the pinhole and simultaneously the alignment of the fiber coupler was optimized by hand (or vice versa). This procedure was uncritical using a multi-mode fiber, but good alignment was rather difficult to accomplish in the case of a single-mode fiber.

To compare Strehl ratio maximization with CE optimization we used adaptation trials with N=4096 iteration steps n (control voltage updates) performed by the *AdOpt* system (n=1,…, N). During the first 2048 iteration steps the voltage output of detector PM1 (that measures the power emergent from the pinhole, which is proportional to the Strehl ratio) is used as feedback signal. Starting from the iteration n=(½N +1)=2049 the system switched to the output voltage of detector PM2 for feedback and thus optimized the fiber coupling efficiency (CE) directly in this second phase of the trial (from n=2049 to n=4096). Because of the stochastic nature of the optimization algorithm we used a large number M of consecutively repeated adaptation trials and calculated average curves for the analysis (typically M=500).

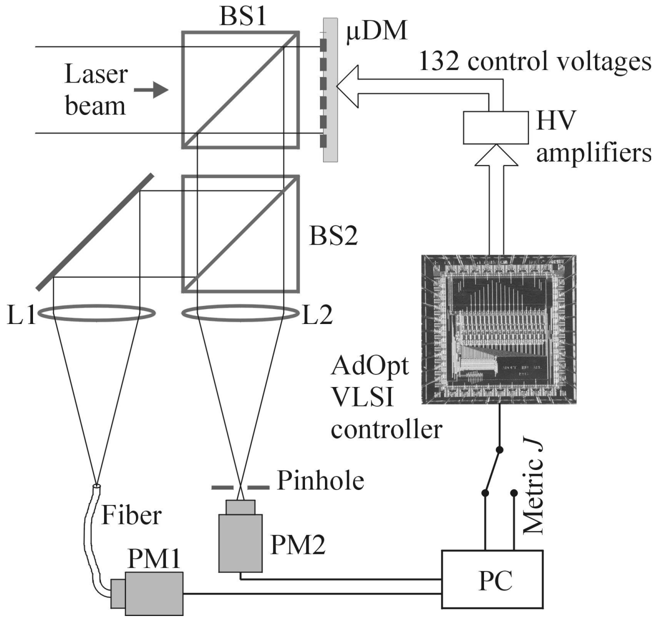

Figure 4: Experimental set-up for comparison of CE optimization and Strehl ratio maximization

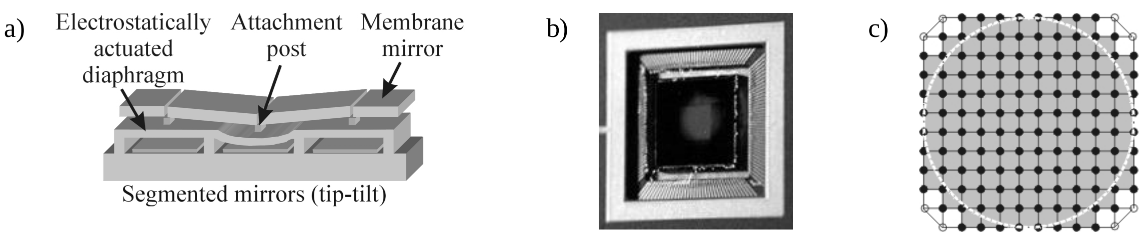

Figure 5: µDM used in the experiments. a) Schematic, b) photograph, c) controlled actuators (filled circles) and controlled part of the mirror membrane (shaded area) in the 132 control channel set-up

4. RESULTS

Experiments for coupling into a multi-mode as well as a single-mode fiber were performed. In case of the graded index multi-mode fiber with a numerical aperture of $NA = 0.275$ the core diameter of the fiber ($d_{\text{fiber}} = 62.5$ µm) is much larger than the diffraction limited focal spot size of a Gaussian beam or a beam with uniform intensity distribution, focused with the same NA value (e.g. 3 µm diameter for the Airy disk of a uniform beam). Thus, there is some degree of freedom to choose the size of the pinhole from the diffraction limit (or less) to the diameter of the fiber core, if lenses with identical focal length are used for both, focusing onto the pinhole and the fiber, and one might expect reasonable coupling efficiency for both cases. Rather than changing the pinhole size in the experiments we used a fixed pinhole diameter of 50 µm, but changed, equivalently, the focal length of the lens L2 (cf. Fig. 4).

Fig. 6a shows the averaged metric evolution curves for the experiments where the focal length of the lenses L1 and L2 were identical. Both curves are normalized to their maximum value observed during the experiments; the numbers should not be mistaken as absolute coupling efficiencies. Optimization of the power emergent from the pinhole (pinhole metric) in the first half of the trial (iterations $n = 1$ to $n = 2048$) allowed only for about 75 % of the maximum value, that was obtained after direct optimization of the power coupled into the fiber in the second half of the trials (iterations $n = 2049$ to $n = 4096$). In this phase of the trial, the power measured in the pinhole decreased by almost 30 %. However, one should be aware that these experimental conditions don't provide a maximization of the Strehl ratio because the diffraction limited spot size is much smaller than the pinhole.

For real Strehl ratio maximization we choose a much larger focal length for L2, in such a way that the pinhole size was smaller than the corresponding Airy disk diameter. The results for the metric evolution curves are shown in Fig. 6b. In this case optimization of the pinhole metric (i.e. Strehl ratio) until iteration $n = 2048$ leads to a considerably higher value of the fiber coupling efficiency than in the previous experiment, but is still only 90 % of the value, that is obtained when optimizing the CE directly. It is noteworthy that in the second phase of the experiments (iterations $n = 2049$ to $n = 4096$) the pinhole metric and thus the Strehl ratio decreases to about 50 % of its maximum value. This indicates, that maximum CE for a multi-mode fiber is not necessarily connected with a maximum Strehl ratio.

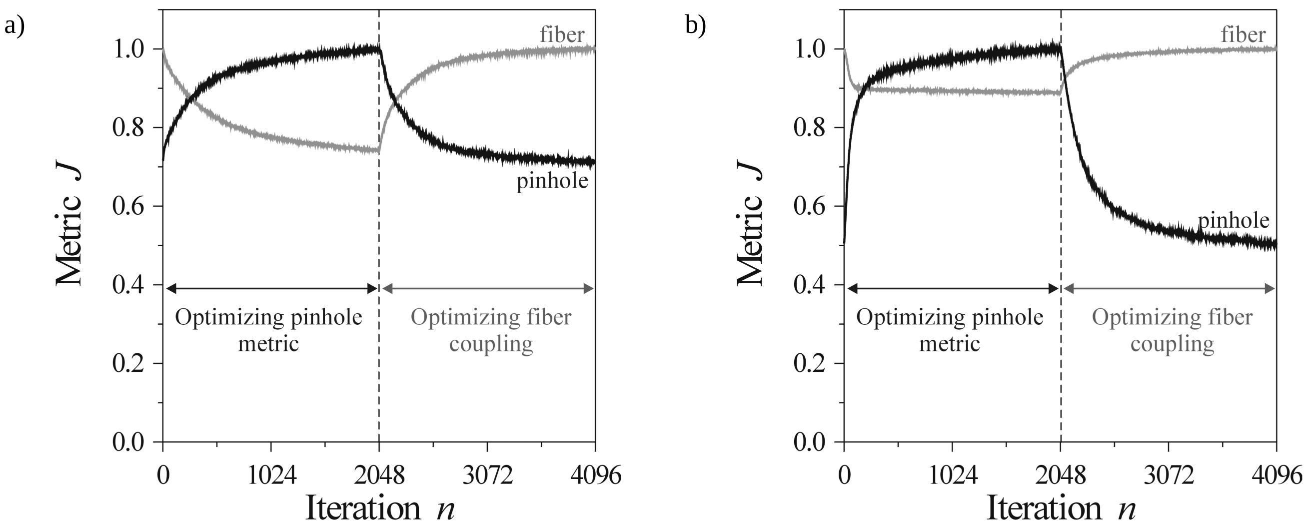

Figure 6: Metric evolution curves of optimization trials for coupling into a multi-mode fiber. a) Focal length of lens $F_{L2} = F_{L1}$; b) $F_{L2} > F_{L1}$

For coupling into a single-mode fiber the focal length of lens L2 was also chosen to provide an Airy disk diameter larger than the pinhole size. The metric evolution curves shown in Fig. 7 indicate a rather large difference between Strehl ratio maximization and CE optimization: Strehl ratio optimization resulted in about 60 % of the maximum coupling efficiency. One has to consider that the system is very sensitive to misalignments even in the sub-µm range, because of the small mode-field diameter (≈ 4 µm) of the single-mode fiber. CE optimization can correct such misalignments and it is unclear to which extent they affected the coupling efficiency during Strehl ratio maximization in the first half of the adaptation trial. However, this shows an important advantage of direct CE optimization: The system is quite insensitivity to misalignments and able to compensate them during operation.

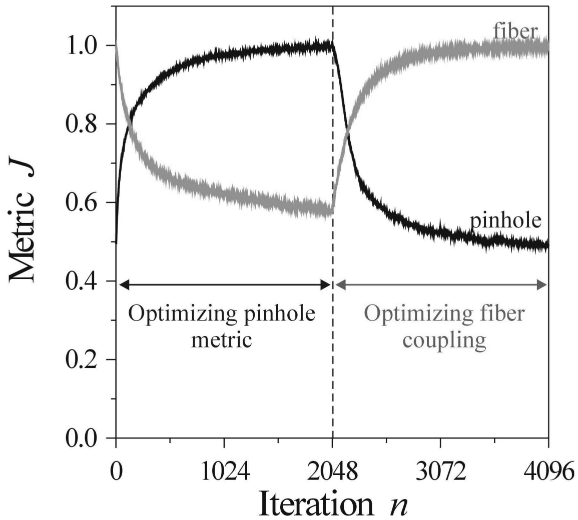

Figure 7: Averaged metric evolution curves for coupling into a single-mode fiber

5. CONCLUSION

Fiber coupling with an adaptive optical system with a 132 control channels was demonstrated. The use of a stochastic parallel gradient descent algorithm for model-free optimization allowed for the direct optimization of the coupling efficiency. Strehl ratio maximization using the same control system to maximize the optical power in a pinhole placed in the focal plane of a focusing lens was used to model a conventional adaptive optics system based on wavefront conjugation. Using the power coupled into the fiber as feedback signal resulted always in a higher coupling efficiency when compared directly with Strehl ratio maximization and revealed much less sensitivity to misalignments of the optical elements. Such adaptive optical fiber couplers may not only be used to compensate atmospheric turbulence effects in fiber-to-fiber free-space communication links but also e.g. as alternative to laboratory fiber couplers based on conventional mechanical alignment.

ACKNOWLEDGMENT

This work was performed while T. Weyrauch held a National Research Council Research Associateship Award at the U.S. Army Research Laboratory.

REFERENCES

1. B. M. Levine, E. A. Martinsen, A. Wirth, A. Jankevics, M. Toledo-Quinones, F. Landers, and T. L. Bruno, "Horizontal line-of-sight turbulence over near-ground paths and implications for adaptive optics correction in laser communication," *Appl. Opt.* **37** (21), 4553-4560 (1998).
2. J. W. Hardy, "Active optics: a new technology for the control of light," *Proc. of the IEEE* **66**(6), 651-697 (1978).
3. J. C. Spall, "A stochastic approximation technique for generating maximum likelihood parameters estimates," in *Proceedings of the American Control Conference* (Institute of Electrical and Electronics Engineers, Piscataway, N. J., 1987), pp. 1161-1167.
4. M. A. Vorontsov, G. W. Carhart, and J. C. Ricklin, "Adaptive phase-distortion correction based on parallel gradient-descent optimization," *Opt. Lett.* **22,** 907-909 (1997).
5. R. T. Edwards, M. Cohen, G. Cauwenberghs, M. A. Vorontsov, and G. W. Carhart, "Analog VLSI parallel stochastic optimization for adaptive optics," in *Learning on Silicon*, G. Cauwenberghs and M. A. Bazoumi, eds. (Kluwer Academic, Boston, Mass., 1999), pp. 359-382.

6. M. A. Vorontsov, G. W. Carhart, M. Cohen, and G. Cauwenberghs, "Adaptive optics based on analog parallel stochastic optimization: analysis and experimental demonstration," *J. Opt. Soc. Am. A* **17**(8), 1440-1453 (2000).
7. T. Weyrauch, M. A. Vorontsov, T. G. Bifano, and M. K. Giles,"Adaptive optics system with micromachined mirror array and stochastic gradient descent controller," in *High-Resolution Wavefront Control: Methods, Devices and Applications II*, Proceedings of SPIE Vol. 4121 (2000), pp. 178-188.
8. T. Weyrauch, M. A. Vorontsov, T. G. Bifano, J. A. Hammer, M. Cohen, and G. Cauwenberghs, "Microscale adaptive optics: wavefront control with a μ-mirror array and a VLSI stochastic gradient descent controller," *Appl. Opt.* **40**(24), 4243-4253 (2001).
9. M. L. Plett, P. R. Barbier, and D. W. Rush, "Compact adaptive optical system based on blind optimization and a micromachined membrane deformable mirror," *Appl. Opt.* **40** (3), 327-330 (2001).
10. C. Ruilier and F. Cassaing, "Coupling of large telescopes and single-mode waveguides: application to stellar interferometry," *J. Opt. Soc. Am. A* **18**(1), 143-149 (2001).